Novelty low-cost integrated photonic biosensor using broadband source and on-chip spectral filter

D. Martens[1,2], A. Stassen[3], W. Van Roy[3], P. Bienstman[1,2]

[1] Photonics Research Group, Ghent University-IMEC, Ghent 9000, Belgium
[2] Centre for Nano- and Biophotonics, Ghent University, Ghent 9000, Belgium
[3] IMEC, Leuven 3001, Belgium

Integrated label-free photonic biosensors provide an excellent limit of detection in combination with a low-cost disposable. Their application has thus far been limited by the necessity of an expensive tunable laser. In this article, we present a novel sensor, eliminating the tunable laser by combining a sensitive Mach-Zehnder interferometer with a broadband light source and an on-chip spectral filter. By curve fitting the original Mach-Zehnder spectrum can be accurately reconstructed from the output of the spectral filter. Bulk sensing experiments yield a limit of detection comparable to conventional integrated photonic biosensors, paving the way for a more widespread range of application.

Introduction

Integrated label-free photonic biosensor are well-equipped for a plethora of applications, as they provide an excellent limit of detection in combination with a low-cost disposable as well as small sample volume [1]. In general, the sensing occurs through the effective index of a waveguide, which is influenced by the immediate environment through the evanescent field. A change in the environment, either a bulk change or a binding event, results in a change in the effective index of the waveguide. This in turn, is translated into a measurable quantity by a photonic transducer, like the ring resonator, the Mach-Zehnder interferometer or a Vernier-cascade which all translate the effective index change specifically to a peak shift [2].
The widespread breakthrough of these structures has hitherto been limited by the optical interrogation mechanism, which generally requires an expensive tunable laser. In this paper, a novel biosensor is presented, avoiding the tunable laser by combining a broadband light source with a very sensitive Mach-Zehnder interferometer photonic transducer and an on-chip spectral filter.

Sensor design

The material platform used for our sensors is silicon nitride. This is preferred over the more conventional silicon on insulator (SOI), as silicon nitride, in contrast with silicon, is transparent in the very near infrared. The sensor can therefore operate in the very near-infrared wavelength range. This spectral region is of particular interest for sensing application due to its negligible water absorption, low fluorescence, the availability of high quality low-cost sources and detectors as well as the presence of the therapeutic window for minimal photo damage to the tissues [3].
To bypass using a tunable laser, this sensor uses a broadband light source in combination with an on-chip spectral filter. An arrayed waveguide grating (AWG) is used as on-chip spectral filter, as it combines a limited footprint with excellent performance [4]. A microscopy picture of such a device is shown in figure 1. Characterization of similar devices in the same Si_3N_4 material platform has yielded an

insertion loss of 1 dB and a crosstalk of 20 dB, rendering these devices state-of-the-art in the given wavelength range [4]. Due to fabrication limitations, the device performance deteriorates slightly when the channel spacing is decreased below 1 nm. For these sensors, 30-channel AWGs with a 1-nm channel spacing are employed.

Due to the AWG channel spacing of 1 nm, a photonic transducer is required that combines a free spectral range of multiple nanometers with a large sensitivity. The Mach-Zehnder interferometer (MZI) is selected, as the spectral period can be determined by carefully selecting the difference in optical path length between both arms. The sensitivity on the other hand, can be increased by extending the arm length of the Mach-Zehnder. To ensure a high sensitivity, one of the Mach-Zehnder arms is isolated by means of a photodefinable silicon oxide cladding, while the other remains uncladded and is therefore exposed to the analyte. Hence, the interferometric effect enhances the shift caused by the analyte, while other effects that affect both arms, like temperature fluctuations, are not enhanced and are therefore comparatively small. An illustration of the complete integrated circuit is shown in figure 2. A photonic transducer that possesses similar qualities and can serve as an alternative is the Vernier cascade, consisting of a cascade of ring resonators [5]. The Mach-Zehnder interferometer is preferred however, as it offers higher power efficiency as well as a more straightforward spectral shape, resulting in an easier and more accurate fitting procedure.

To couple light from and to the chips, grating couplers are used. In the given material platform, these have a coupling loss around 6 dB per grating coupler [6]. A vertical coupling mechanism is used, as this allows coupling light anywhere on the surface, rather than only at the edges. This strongly increases the potential for multiplexing, as each sensor has numerous outputs which need to be monitored.
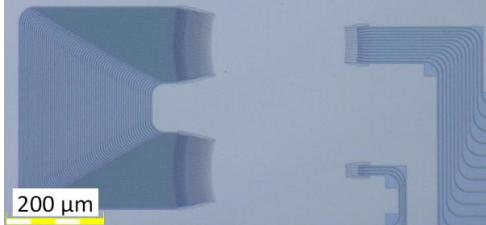
Figure 1: Microscopy image of silicon nitride arrayed waveguide grating
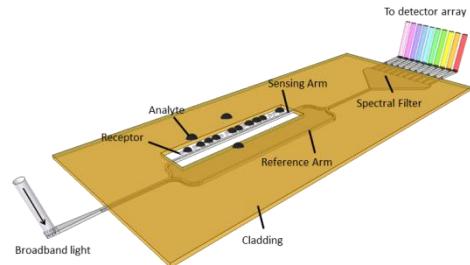
Figure 2: Integrated photonic network

Fitting procedure

The effective refractive index is tracked by observing changes in the peak wavelengths of the cosine shaped Mach-Zehnder spectrum. The spectral period of the sensor is typically 7-10 nm, resulting in 3-4 peaks within the free spectral range of the arrayed waveguide grating. A highly accurate fitting of these peaks is vital in achieving an adequate limit of detection, as it allows improving the minimum detectable wavelength shift by multiple orders of magnitude over the channel spacing of the arrayed waveguide grating. The procedure needs to be robust as typically only 5-10 points are available per peak and those are furthermore prone to experimental noise.

Due to the limited amount of data available per wavelength peak, a fit function with limited parameters is used, in the form of a high order Taylor approximation of a cosine function around the peak. This is most accurate around the peak, while there is an

intrinsic error on the outer points. To mitigate this as well as avoid discontinuities upon edge points drifting in and out of range, weights are added to the fit, favoring high intensity points over their low intensity counterparts.

Bulk limit of detection

To characterize these sensors, a setup mimicking a point-of-care sensing device was used. As an optical input, a free-space 12 mW SLED centered around 850 nm was used, hanging centimeters above the sample. The light was brought onto the grating couplers through flood illumination, corresponding to a light spot multiple orders of magnitude larger than the input grating couplers. The means that alignment conditions are strongly less stringent compared to coupling through an optical fiber. Outputs were monitored through a CMOS camera.

To determine the bulk sensitivity of the sensors, multiple types of phosphate-buffered saline with a known refractive index were brought onto the sample through in-house fabricated Polydimethylsiloxane (PDMS) microfluidic channels. These fluids were alternated with water to bring the wavelength back to the baseline.

Numerous experiments were executed, in figure 3 the time evolution of the peaks in one of them is displayed, where the types of PBS as well as the refractive index difference with water are indicated. The different colors correspond to different peaks of the same sensor; hence their shifts in reaction to the same analyte are approximately equal. Upon switching back to water after application of PBS, the signal returns almost completely back to the baseline. The small deviation is most likely related to temperature drift throughout the experiment.
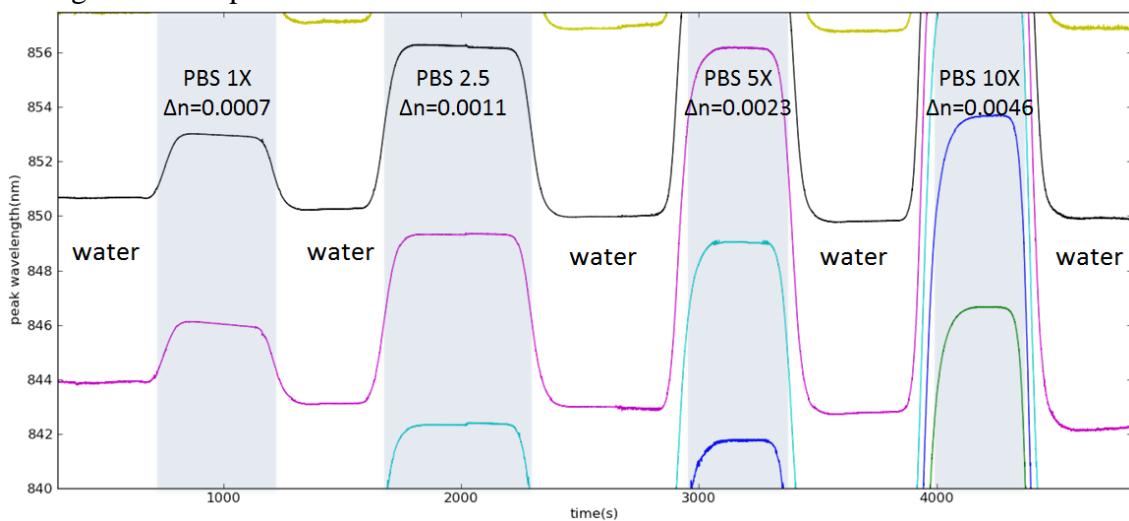
Figure 3: Time evolution of fitted peak wavelengths of Mach-Zehnder interferometer upon exposure of different PBS mixtures alternated with water. Different colored curves correspond to different peaks of the same sensor. The refractive index difference with water of the mixtures is indicated on the figure.

To evaluate a sensor, a common figure of merit is the limit of detection. The limit of detection is determined by the ratio of the minimum detectable wavelength shift and the sensitivity. The minimal detectable wavelength shift is defined as 3 times the standard deviation on the signal in an interval where it is expected to be constant. For this sensor, the minimal detectable wavelength shift was found to be 4 pm, after averaging and after correcting for linear drift.

The sensitivity is extracted by fitting the changes in peak wavelength linearly to the changes in bulk effective index. The slope of this line through the origin is the

sensitivity. For this experiment such a linear fit is shown in figure 4. The experimental data matches the fit very well. There is a slight deviation on the first point, most likely related to an inaccurate concentration of analyte, as it was recurring throughout multiple experiments. This linear fit yields a sensitivity of 5440 nm/RIU.

These values provide a limit of detection of $7*10^{-7}$ RIU, a result comparable to most similar, more expensive sensing mechanisms.
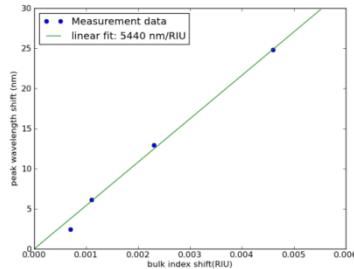
Figure 4: Linear fit of the peak wavelength shift to the bulk index shift

Conclusion

A novelty integrated photonic sensor was presented, configured for point-of-care detection in numerous ways. Through usage of a broadband light source in combination with an on-chip spectral filter, an expensive tunable laser is no longer necessary. The broadband light source is furthermore used in flood illumination, resulting in less stringent alignment conditions. The different outputs of the spectral filter are monitored, and through the curve fitting the peak wavelengths of the original spectrum are accurately determined. Despite the less trivial interrogation mechanism, an impressive limit of detection of $7*10^{-7}$ RIU is achieved, paving the way for numerous applications.

Acknowledgement

References

[1] A. Subramanian, E.M.P. Ryckeboer, A. Dhakal, F. Peyskens, A. Malik, B. Kuyken, H. Zhao, S. Pathak, A. Ruocco, A. De Groote, P.C. Wuytens, D. Martens, F. Leo, W. Xie, U.D. Dave, M. Muneeb, Pol Van Dorpe, Joris Van Campenhout, W. Bogaerts, P. Bienstman, N. Le Thomas, D. Van Thourhout, Zeger Hens, G. Roelkens, R. Baets, "Silicon and silicon nitride photonic circuits for spectroscopic sensing on–a–chip ", Photonics Research, vol. 5, B47-B59, 2015

[2] T. Claes, W. Bogaerts, P. Bienstman, "Experimental characterization of a silicon photonic biosensor consisting of two cascaded ring resonators based on the Vernier-effect and introduction of a curve fitting method for an improved detection limit", Optics Express, vol. 18, 22747-22761, 2010

[3] A. Subramanian, P. Neutens, A. Dhakal, R. Jansen, T. Claes, X. Rottenberg, F. Peyskens, S. Selvaraja, P. Helin, B. Du Bois, K. Leyssens, S. Severi, P. Deshpande, R. Baets, P. Van Dorpe, "Low-loss singlemode PECVD silicon nitride photonic wire waveguides for 532-900 nm wavelength window fabricated within a CMOS pilot line", IEEE Photonics Journal, vol. 5, p.2202809, 2013

[4] D. Martens, A. Subramanian, S. Pathak, M. Vanslembrouck, P. Bienstman, W. Bogaerts, R. Baets, "Compact Silicon Nitride Arrayed Waveguide Gratings for Very Near-infrared Wavelengths", Photonics Technology Letters, vol. 27, 137-140, 2015

[5] T. Claes, W. Bogaerts, P. Bienstman, "Vernier-cascade label-free biosensor with integrated arrayed waveguide grating for wavelength interrogation with low-cost broadband source", Optics Letters, vol. 36, 3320-3322, 2011

[6] A. Subramanian, S. Selvaraja, P. Verheyen, A. Dhakal, K. Komorowska, R. Baets, "Near infrared grating couplers for silicon nitride photonic wires", IEEE Photonics Technology Letters, vol. 24, 1700-1703, 2012